Proceedings of ASME Turbo Expo 2011
GT2011
June 6-10, 2011, Vancouver, British Columbia, Canada

GT2011-45426

DESIGN OF TWO COUNTER-ROTATING FAN TYPES AND CFD INVESTIGATION OF THEIR AERODYNAMIC CHARACTERISTICS

Xiao-He Yang **Peng Shan**
School of Jet Propulsion, Beijing University of Aeronautics and Astronautics
Beijing 100191, P. R. China
Email: xiaocao710181@163.com Email: PShan@buaa.edu.cn

ABSTRACT

The design information and numerical investigation are presented for two kinds of counter-rotating fans. The fans, both vaneless and non-aspirated, are intended for a civil aviation engine with a bypass ratio of 8 and for a military engine with a bypass ratio of 0.5 respectively. The pressure ratios are respectively 1.60 and 3.50, and the tip speeds are (300 m/s, -222 m/s) and (500 m/s, -391 m/s). The design rotating speed ratio of the front to the aft rotor is discussed based on one-dimensional analysis. The variations in pressure ratios, isentropic efficiencies, diffusion losses and shock losses at mean-line with the design rotating speed ratios are studied. The flow fields of the two contra-stages are numerically simulated and the detailed flow physics is investigated at both design and off-design conditions. The simulations reveal that the two stages both perform well. The civil engine contra-stage test fans are still conventional transonic rotors due to the low pressure ratio and low tip speeds. For the military engine contra-stage, the aft rotor differs from the conventional transonic front rotor. It is a full-span relative supersonic rotor in which both the leading edge shock and the passage shock extend from the casing to the hub. At the stall point, for the low pressure ratio civil test fan, both the front and aft rotors are stalled and the shocks detached. In the corresponding high pressure ratio military fan, only the aft rotor is stalled which determines the stage stall point.

NOMENCLATURE

C	Absolute Velocity
L_u	Shaft work input per unit mass flow
L_f	Lost work per unit mass flow
M	Mach number
U	Local rotor circumferential speed
W	Relative Velocity
Ω	Degree of reaction

Subscripts

1, 2, 3, 4	Inlet, outlet of the front and aft rotor
C	Absolute
W	Relative
F	Front rotor
A	Aft rotor
CS	Contra-stage
Ml	Mean-line

Abbreviation

CFD	Computational Fluid Dynamics
CRF	Counter-Rotating Fan
CRP	Counter-Rotating Propfan

INTRODUCTION

For civil aviation engines, a lower specific fuel consumption and a lower noise level are desired. It is well known that a larger bypass ratio implies a higher propulsive efficiency and a limited fan tip speed translates into a lower noise level. Further increasing of the bypass ratio means a higher fan mass flow at a lower fan pressure ratio. The reduction of fan pressure ratio and the limitation of fan tip speed will reduce the rotational speed of the low pressure spool, which results in both a larger diameter and a larger stage number of the low pressure turbine component with a lower turbine efficiency, while additionally a larger shaft diameter is required due to a higher torque to transfer. This speed mismatch problem between the fan and low pressure turbine will become unacceptable if the bypass ratio is beyond

10. However some new engine layouts and transmission schemes conceivably allow this. One possible high-potential technology is the counter-rotating fan (CRF) driven by either a gearbox or a counter-rotating turbine. In the other development direction, for military engines, a high thrust-weight ratio is emphasized to pursue high acceleration, maneuverability, payload, and supersonic cruise, which leads to more compact and lighter engines. For those objectives, focus is predominantly on increasing tip speed and improving blade shapes suitable for transonic and supersonic flow conditions. The loading level of axial-flow compressors has made significant progress. A notable milestone is the stage designed by Wennerstrom in 1970s [1], passing 195 kg/(s.m^2) based on frontal area, producing a pressure ratio of 1.95 at 457 m/s tip speed with a peak isentropic efficiency over 88%. In the decades after that, no significant developments have been made on these conventional stages. A conventional stage producing a pressure ratio of 3.0 has not been achieved. Higher loading levels are always coupled with a lower efficiency and a decreased stall margin. Meanwhile, the unconventional stages, intended for military applications, incorporating innovative configurations, such as counter-rotating stages, splitters [2], aspirated and blowing blades [3], tandem blades [4], etc. have evolved substantially. Relative to a conventional stage, the counter-rotating stage exhibits structural and aerodynamic advantages. Structurally, the counter-rotating configuration is axially shorter, more compact and lighter, due to the elimination of stators. Aerodynamically, the aft rotor takes advantage of the circulation from the front rotor, which translates into an increased relative speed, thus an increased loading level, with a lower mechanical speed. To summarize, the application of counter-rotating can be divided into two categories, low-speed, low-pressure-ratio civil fans, met with great success, and high-speed, high-pressure-ratio stages, met with limited success because of the inevitable increase of relative Mach number into the aft rotor.

The concept of CRF was proposed by Young who analyzed its basic principle (1951, [5]). At that time, Johnsen and Fessler designed an isolated transonic rotor in front of which the guide vanes were placed to produce counterswirl (1957, [6]). Pratt and Whitney Aircraft reported a three-stage axial compressor (1966, [7]), of which the second stage was a full-span relative supersonic compressor resulting from counterswirl in the approaching air. This stage was designed to produce a pressure ratio of 2.75 with a relatively low tip speed of 295 m/s, but the measured stage isentropic efficiency did not exceed 70% at design speed. Curtiss-Wright attempted, unsuccessfully, to design a highly loaded counter-rotating compressor intended for a supersonic aircraft (1957, [8, 9]). Wennerstrom reviewed this design and pointed out that the exceptionally high diffusion of its aft rotor with no control of its boundary layer led to failure [10]. An extensive assessment of the performance improvement for a single stage fan with inlet counter-swirl was made by Law and Wennerstrom (1987, [11]). The stage was designed to produce a pressure ratio of 2.264 with an isentropic efficiency of 86.8%. Apart from the diffusion level which was constrained to proven levels, suitable airfoils developed for high Mach numbers were also a reason for its success. Sharma investigated the aerodynamics and aeroacoustics of CRF based on experimental work [12]. After 2000, Kerrebrock combined aspirated flow control with a counter-rotating to design an aspirated CRF [13]. Experimental tests confirmed a pressure ratio of 2.9 at an 89% isentropic efficiency at the design speed. A Mach 2.4 transport engine with two supersonic through-flow counter-rotating fan rotors was reported by Donald [14]. In addition Ryojiro Minato developed a CRF for supersonic unmanned plane [15].

As early as the second world war, counter-rotating propellers driven by piston engines emerged. It provides a higher propulsive efficiency due to swirl-free exit flow and the gyroscopic couple is greatly reduced which enhances the flight performance. In the mid 70's, a new propulsor, the so-called propfan ranging between a conventional propeller and a turbofan was proposed and investigated. Various kinds of counter-rotating propfan (CRP), aimed at increasing the bypass ratio of the civil engine to reduce the specific fuel consumption and noise level, were extensively researched and pronounced progress was made, including ducted and unducted, gear-driven and counter-rotating turbine driven CRP. In the past decades, technical programs of CRF/CRP in different nations have been carried out in terms of aerodynamics, aeroacoustics, aeroelasticities, installation and transmission, also numerous patents were applied. GE and NASA developed the gearless unducted CRP GE36. Allison and PW designed geared unducted CRP 578-DX. Rolls-Royce proposed geared unducted CRP RB509 and gearless ducted CRP (or CRF) RB529. Germany MTU developed geared Counter-Rotating Integrated Shrouded Propfan (CRISP). Russia proposed geared unducted CRP D27 and ducted CRP HN93 which were applied to AN70 and TU204 respectively. GE also developed CRF after 2000. SNECMA developed CRF under VITAL program. Basically, the ducted CRP or CRF is regarded as a particularly attractive propulsor to implement underwing mounted very high bypass ratio engine based on size and acoustic limitations.

Conventionally, a stage is defined as a rotor blade row followed by a stator vane row. The function of the aft rotor of CRF is in common with a stator which turns the flow back to the axial direction, with the difference that the former introduces work as well as the front rotor of CRF and the latter does not. From this point of view, a front rotor combined with an aft rotor of CRF is defined as a contra-stage in this paper. Two contra-stages, both vaneless and non-aspirated, were designed and numerically investigated. They are intended for a civil aviation engine with a bypass ratio of 8 and for a military engine with a bypass ratio of 0.5 respectively, corresponding to the low-speed and high-speed applications of CRF respectively. The pressure ratios are respectively 1.60 and 3.50, and the tip speeds are (300 m/s, -222 m/s) and (500 m/s, -391 m/s). The exit flows of both contra-stages are swirl free.

AERODYNAMIC DESIGN OF TWO CRF TYPES

The aerodynamic design parameters of the civil fan with low tip speeds, and the military fan with high tip speeds are presented in Table 1. The civil fan is a 0.402 scale test fan passing a mass flow of 102.0 kg/s with a stage pressure ratio of 1.60. The military fan is a full scale fan passing a mass flow of 64.4 kg/s with a stage pressure ratio of 3.50. The aspect ratio is defined upon the mean rotor span and the average of axial length of blade sections.

In a conventional rotor-stator stage, the reaction degree reflects the fraction of stage static pressure rise which occurs through the rotor and stator. Firstly, similar to the reaction of a conventional stage, this paper defines the reactions of the front and aft rotor of a contra-stage as

$$\Omega_F = \frac{1}{L_{u,F}}\left(\int_1^2 \frac{dp}{\rho} + L_{f,F}\right) = \frac{1}{L_{u,F}}\left(L_{u,F} - \frac{C_2^2 - C_1^2}{2}\right),$$

$$\Omega_A = \frac{1}{L_{u,A}}\left(\int_3^4 \frac{dp}{\rho} + L_{f,A}\right) = \frac{1}{L_{u,A}}\left(L_{u,A} - \frac{C_4^2 - C_3^2}{2}\right) \qquad (1)$$

$$L_{u,F} = \frac{W_1^2 - W_2^2}{2} + \frac{U_2^2 - U_1^2}{2} + \frac{C_2^2 - C_1^2}{2},$$

$$L_{u,A} = \frac{W_3^2 - W_4^2}{2} + \frac{U_4^2 - U_3^2}{2} + \frac{C_4^2 - C_3^2}{2} \qquad (2)$$

For a contra-stage with swirl-free exit flow, it is noticed that the reaction of the aft rotor must be greater than 1.0, because the outlet absolute velocity C_4 is lower than C_3. Secondly, considering the physical meaning of reaction, this paper defines the reaction of a contra-stage Ω_{cs} as

$$\Omega_{CS} = \frac{1}{L_{u,F} + L_{u,A}}\left(L_{u,F} - \frac{C_2^2 - C_1^2}{2}\right) \qquad (3)$$

Further, in condition of swirl-free inlet and exit flow, the works of rotors are

$$L_{u,F} = \omega_F C_u R\,, \quad L_{u,A} = \omega_A C_u R \qquad (4)$$

where ω is shaft angular velocity and $C_u R$ is outlet circulation of the front rotor. It follows that

$$\Omega_{CS} = \Omega_F \frac{H}{H+1} \qquad (5)$$

where H is the rotating speed ratio of the front to the aft rotor. So the reaction of a contra-stage is a function of the front rotor reaction and the rotating speed ratio.

The two reaction definitions described above have different meaning. The former represents the ability of the rotor to convert the shaft work into static pressure rise, while the latter expresses the static pressure rise distribution between the front and aft rotor. As the air flows across the aft rotor, not only the relative velocity but also the absolute velocity decreases. The change of absolute velocity is different from a conventional rotor but similar to a stator.

Table 1. Preliminary design parameters of the civil and military contra-stages

	Civil rotors		Military rotors	
	Front	Aft	Front	Aft
Tip speed (m/s)	300	-222	500	-391
Total pressure ratio specification	1.328	1.205	2.170	1.613
Flow per frontal area kg/(s,m^2)	200.9	-	184.9	-
Flow per annulus area kg/(s,m^2)	220.8	-	203.1	-
Flow coefficient $\phi = C_{Z,Ml}/U_{Ml}$	1.029	-	0.535	-
Work coefficient $\psi = L_u/U_{Tip}^2$	0.289	0.396	0.322	0.422
Reaction, defined as equation (1)	0.911	1.489	0.682	1.323
Reaction, defined as equation (3)	0.521	-	0.379	-
Hub-tip ratio	0.300	0.433	0.300	0.596
Mean-line diffusion factor	0.417	0.351	0.506	0.414
Hub relative Mach	0.681	0.892	0.754	1.534
Tip relative Mach	1.165	1.219	1.636	1.593
Blade count	16	19	18	21
Average solidity	1.290	1.581	1.970	1.856
Average aspect ratio	2.216	1.851	1.746	1.536

Different from conventional rotor-stator stages, the CRF presents one more design freedom to choose, the rotating speed ratio of the front to the aft rotor. Due to the elimination of the stators, the relative Mach number at the full-span inlet of the aft rotor is substantially higher than conventional rotors, which tends to increase the shock loss and deteriorate the shock-boundary layer interaction. Lowering the rotating speed of the aft rotor is beneficial to decrease the shock loss, but at an increase of work coefficient and diffusion level. The effect of the speed ratio on the contra-stage performance is modeled and investigated with a component overall design code and a one-dimensional mean-line analysis program. The losses were defined by the sum of diffusion losses plus shock losses, with the former defined by Lieblein empirically as a function of diffusion factor [16] and the latter by the Miller, Lewis and Hartmann normal shock model [17]. The cross-sectional-area change is also taken into account. Taking the civil CRF for instance, under the condition of constant stage pressure ratio 1.60 and the front rotor tip speed 300 m/s, the variation in total pressure ratios, shock losses, diffusion losses, and isentropic efficiencies with the rotating speed ratio at the mean-line are shown in Fig. 1 through 3 respectively. The abscissa, rotating speed ratio, is defined as ω_F / ω_A . It is indicated that most of the losses result from the aft rotor. As the rotating speed of the aft rotor increases, its total pressure ratio rises and its shock loss and diffusion loss both increase rapidly. Meanwhile, the total pressure ratio of the front rotor decreases with a slightly drop in shock loss and a nearly constant diffusion loss. The efficiency of the front rotor slightly drops due to the decrease in the total pressure ratio and the negligible variation in total losses, compared with quite a marked drop in efficiency of the aft rotor and consequently the contra-stage. The speed ratio of the front to the aft rotor ultimately chosen is 4:3 to ensure a prominent civil CRF efficiency. As illustrated in Fig. 4 through 6, the military contra-stage exhibits similar tendencies to that of the civil contra-stage, with more precipitous changes in losses of the aft rotor, consequently the efficiencies. Hence, as the rotating speed of the aft rotor rises to an extent, the front rotor has to produce a higher pressure ratio to compensate the aft rotor losses, which means the variation in the pressure ratios with the speed ratio is no more monotonic as that of the civil contra-stage.

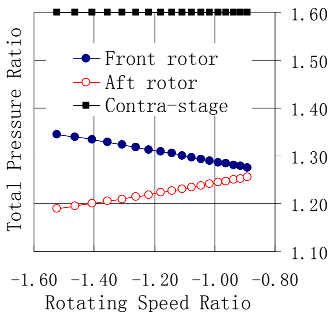

Fig. 1 Variation in pressure ratios of two civil fan rotors with speed ratio

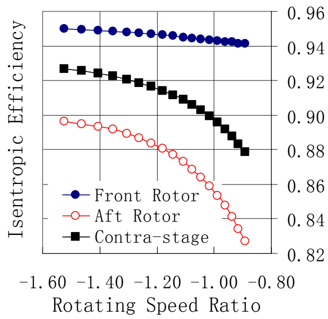

Fig. 2 Variation in isentropic efficiencies of two civil fan rotors with speed ratio

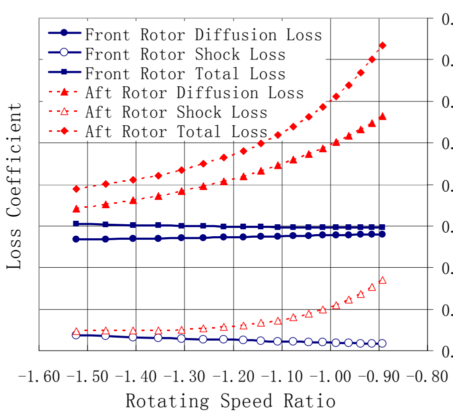

Fig. 3 Variation in shock losses, diffusion losses, and total losses of two civil fan rotors with speed ratio

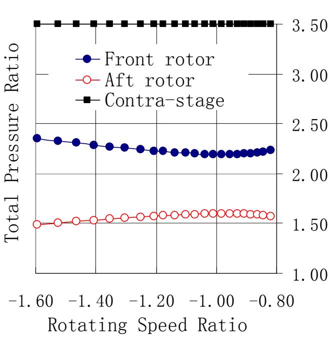

Fig. 4 Variation in pressure ratios of two military fan rotors with speed ratio

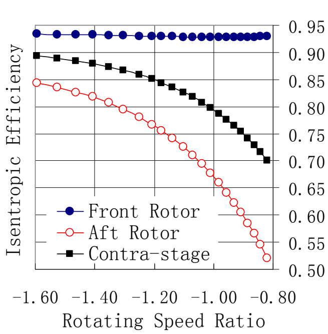

Fig. 5 Variation in isentropic efficiencies of two military fan rotors with speed ratio

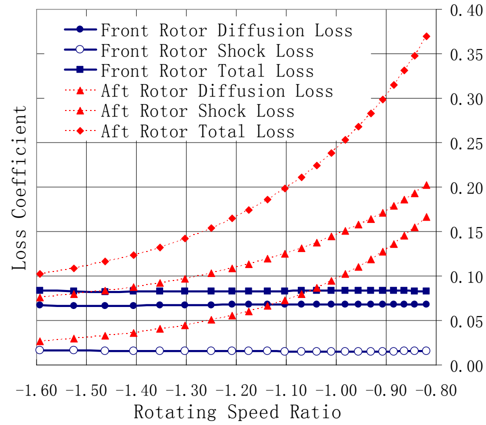

Fig. 6 Variation in shock losses, diffusion losses, and total losses of two military fan rotors with speed ratio

The detailed aerodynamic design of the two contra-stages was accomplished employing a through-flow inverse design code based on the stream-line curvature method [18], and a blading code based on the arbitrary-shape camber line airfoil formatting method [19]. The through-flow design assumes the flow is axisymmetric and described by a series of concentric stream tubes across which no mass, momentum, or energy is transported. The code simultaneously solves the full radial equilibrium version of momentum equation and the continuity equation through an iterative numerical procedure at each computing station in sequence, which can be defined by an arbitrary curvilinear path. For the computations located within blade/vane rows, blade force terms are included in the momentum equation as a body-force field assumed to act normal to the blade/vane surface. Entropy gradients are also included, and the losses are estimated in a similar way to that of the mean-line analysis program described above. Arbitrary airfoils are employed for each rotor. Details of the formulation and program are given in [18]. The iterations between the through-flow design and blading were carried out until the design objectives were matched.

After that, a three-dimensional steady viscous CFD simulation was performed to predict the design objectives. The aforementioned design process was repeated to achieve the design specifications.

The mid-streamline elements and Mach number vector diagrams are presented in Fig. 7. The velocity triangles of the two contra-stages are illustrated in Fig. 8.

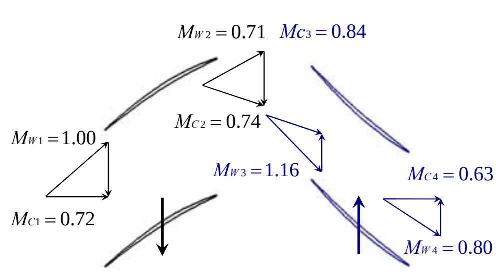

(a) Civil contra-stage

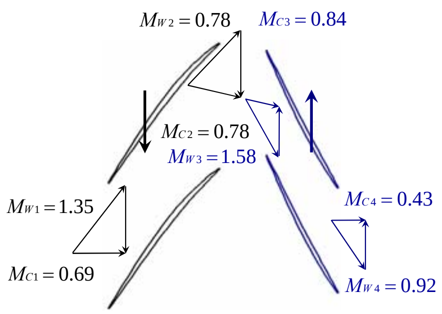

(b) Military contra-stage

Fig. 7 Mid-streamline elements and Mach number diagrams from through-flow inverse design

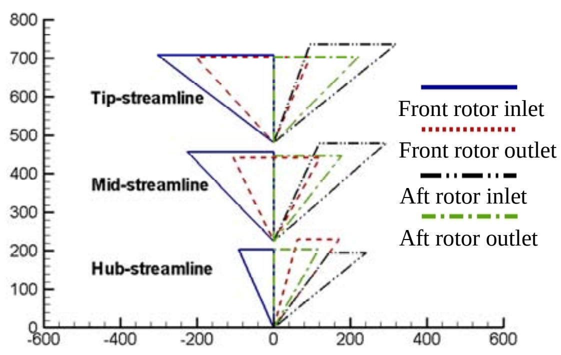

(a) Civil contra-stage

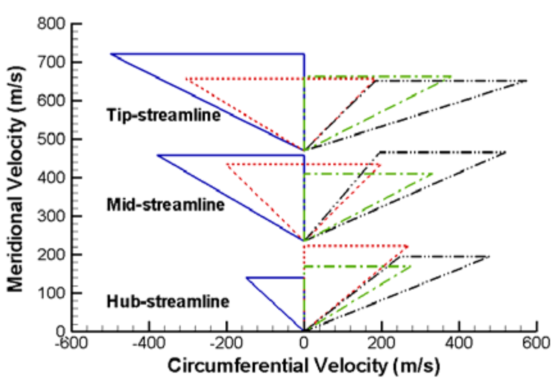

(b) Military contra-stage

Fig. 8 Velocity triangles of the front and aft rotors from through-flow inverse design

Enabled by counter-rotating, the aft rotor of CRF has a relatively lower rotating speed, thus a relatively higher work coefficient compared to the front rotor and a state-of-the-art conventional transonic rotor. It is notable that the circumferential velocity is highest at the outlet of the front rotor. So, according to the radial equilibrium equation, the static pressure at the casing is higher than that at the hub to balance the centrifugal force. Differently, the aft rotor reduces the swirl and turns the flow back to the axial direction, so downstream of the aft rotor the radial gradient in static pressure is much smaller than upstream of it. As a result, the static pressure rise across the aft rotor hub is necessarily higher than that at the casing, and is also notably higher than that across a conventional stator due to the total pressure rise across the aft rotor. Hence the hub of aft rotor is the most likely location where separation occurs in a contra-stage. Keeping this in mind, a local convex hub contour with a positive curvature across the aft rotor is utilized for the purpose of accelerating the flow to avoid separation. The meridional flowpaths of the two contra-stages are shown in Fig. 9 and 10 respectively.

Beneficial from the low total pressure ratio and low wheel speed, the aft rotor of the civil CRF is still a conventional transonic rotor. At the hub, the rotating speed is so low that the total pressure ratio there was decreased to unload the hub sections, which also decreases the inlet Mach number at the hub and alleviates the tendency to choke there. In comparison with a conventional rotor-stator stage with the same level of pressure ratio, the contra-stage provides a higher throughflow capacity. For example，the meridional average Mach number in front of the civil CRF is 0.7022. The capacity leads to a smaller diameter fan, consequently facilitates engine nacelle design and engine installation. This advantage will be more prominent as the bypass ratio increases. Despite the high inlet axial velocity, the relative Mach number at the aft rotor entry is low enough resulting from the low rotating speed, varying from 1.22 at the tip to 0.89 at the hub, in the range of which shock usually represents quite an efficient compression system. High throughflow associated with low whirl speed result in a remarkably high flow coefficient Φ=1.029 at the pitch-line radius of the inlet, which is particularly higher than a conventional rotor-stator stage. The flowpath and blade rows of the civil CRF are shown in Fig. 9 with obviously low stagger angles because of the unconventionally high flow coefficient. As indicated also, the hub sections of the front rotor are close to the axial direction.

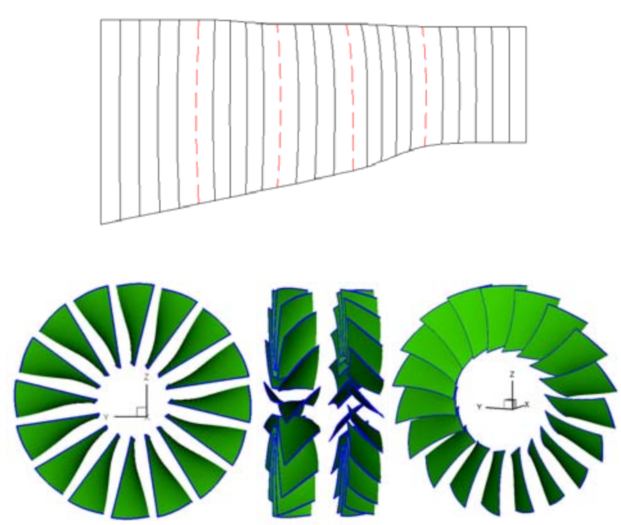

Fig. 9 Flowpath, front and aft blade rows of the civil CRF

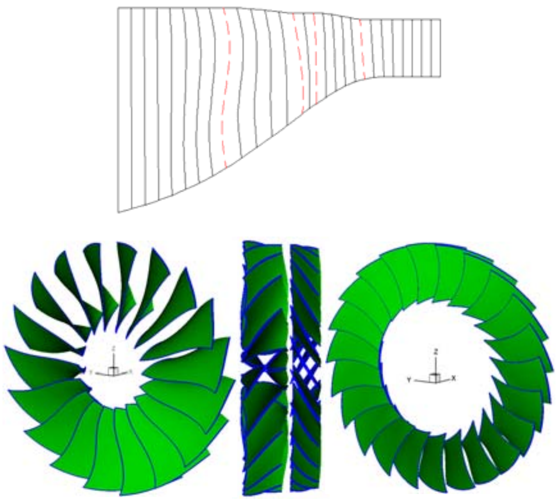

Fig. 10 Flowpath, front and aft blade rows of the military CRF

The flowpath and blade rows of the military CRF are pictured in Fig. 10. In contrast to the aforementioned civil contra-stage and a conventional rotor-stator stage, the aft rotor of the military contra-stage is relatively supersonic from hub to casing due to the high design pressure ratio of 3.50 and the stator elimination. The relative Mach number of the aft rotor at the tip is nearly 1.6, with that at the hub up to 1.5, which incurs high shock loss. For the objective of reducing the shock loss, firstly, the design inlet axial Mach number was conservatively chosen, that is to say not higher than that of a rotor-stator stage with the same pressure ratio level. Secondly, the casing flow path was sloped at -8 degrees across the aft rotor to unload the tip sections. Therefore a local concave tip contour was formed at the leading edge to decrease the Mach number, and a convex tip contour at the trailing edge to alleviate the choke tendency. Thirdly, under the stress limitation, the maximum thicknesses of the aft rotor at the hub were slightly reduced and after-positioned compared to that of conventional transonic rotors. The resultant aft rotor blade maximum thickness varied parabolically from 6.0% chord at the hub to 2.0% chord at the tip, and the chord location of maximum thickness varied linearly from 60% chord at the hub to 70% chord at the tip. The last but not the least, the tip of the aft rotor leading edge was swept forward. Also, a compound forward-swept leading edge was applied to the front rotor to decrease the shock loss and to increase the stall margin.

NUMERICAL SIMULATION AND DISCUSSION OF THE PERFORMANCE AND FLOW FIELDS OF TWO CRF TYPES

Based on the Reynolds averaged Navier-Stokes equations, the 3D steady viscous flow fields of the two contra-stages were simulated employing the commercially available CFD software FINE^{TM} Turbo by NUMECA International.

The governing equations are solved in the relative frame with a cell-centered finite volume formulation. Jameson's second-order central scheme with 2nd and 4th order artificial viscosity is used for the discretization of the convection terms and the central differencing is used for the diffusion terms. Time integration is based on an explicit four-stage Runge-Kutta scheme. The conservative coupling by ptichwise rows approach is used at the interface of the front and aft rotor [20], which provides an exact conservation of mass flow, momentum and energy through the interface. Turbulence closure is achieved using one equation Spalart-Allmaras turbulence model [21]. Implicit residual smoothing, variable time steps, and three-level multigrid are used to accelerate convergence. The HOH-type topology structure grid is employed for both the civil and military contra-stages. Nine grid cells of Butterfly-type topology structure are set within the tip clearance and 69 points are set in the span-wise direction. The total grid point numbers are 682,464 and 629,832 for the front and aft rotor of the civil contra-stage respectively, and are 658,075 and 653,723 for that of the military contra-stage. The distance between the wall and the first node is imposed such that y^+ is less than 2. Checks have shown that the overall performance is not appreciably different if 1.6 times as many grid points are used, and the percentage discrepancies of mass flow, efficiency, and pressure ratio are less than 0.15% for both contra-stages. The computational grids of the two contra-stages are shown in fig. 11 and 12 respectively. The inlet boundary condition consists of the inlet total pressure, total temperature and flow angle. There is no inlet swirl, and the inlet total pressure and temperature were assumed to be uniform. The outlet boundary condition was exit tip static pressure level. All wall boundary conditions were modelled as no-slip and adiabatic.

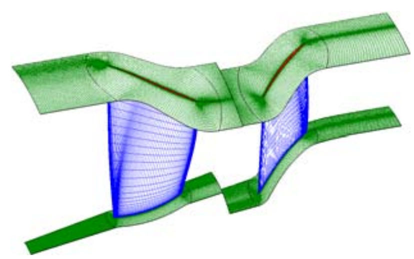

Fig. 11 Computational grids of the civil contra-stage

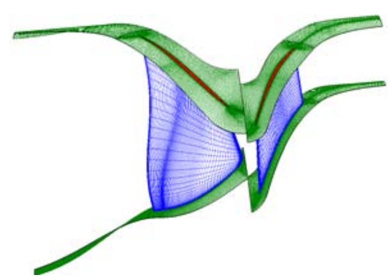

Fig. 12 Computational grids of the military contra-stage

For the scaled civil contra-stage, the tip clearances of the front and aft rotors are both taken as 1.0 mm, equivalent to 0.376% and 0.484% of each rotor mean span respectively. The map of this contra-stage performance is presented in Fig. 13. It is illustrated that this contra-stage has a considerably high efficiency and stall margin. At the design point, this contra-stage passes a flow rate of 102.2 kg/s with a pressure ratio of 1.608, achieving an isentropic efficiency of 91.2%, alternatively a polytropic efficiency of 91.8%, at a stall margin of 18.9%. Correspondingly, the isentropic efficiencies of the front rotor and aft rotor are 93.9% and 88.4% respectively, in good agreement with the one-dimensional code prediction. The peak isentropic efficiency of this contra-stage is 91.9%, corresponding to a polytropic efficiency of 92.3%, with a pressure ratio of 1.489 at (0.95, -0.95) speed. Bearing in mind that the scaled CRF is designed to pass 1/6 mass flow of the full scale CRF, it is reasonable to believe that the full scale CRF will present an even more prominent performance. The relative Mach number distributions at the design point are plotted at 10, 50, and 90% of the span as indicated in Fig. 14. Due to the low rotating speed and conservative loading level, the front rotor exhibits only a weak leading edge shock without passage shock at the tip section, and barely the local supersonic flow and shock are formed at the middle section, while the hub section is a low-staggered subsonic element. Contrastively, at the tip and middle sections, the aft rotor shows a dual-shock structure defined as a leading edge shock followed by a normal passage shock, and still the hub section is a subsonic element. Narrow wake regions are presented also in Fig. 14. It is the shock system described, low diffusion and stators elimination that account for the respectable efficiency achieved by this CRF.

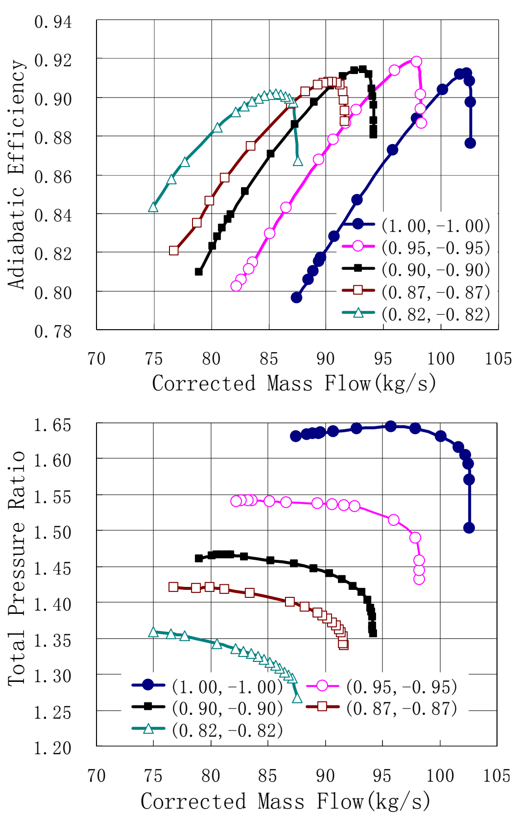

Fig. 13 Corrected civil contra-stage performance map

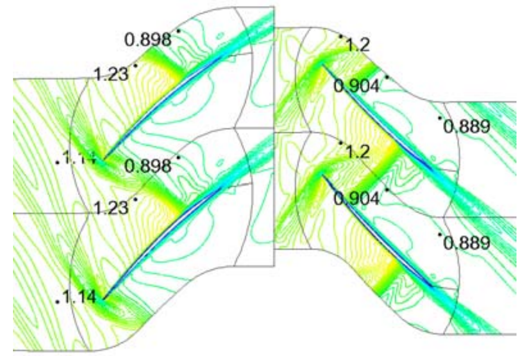

(a) 90% span

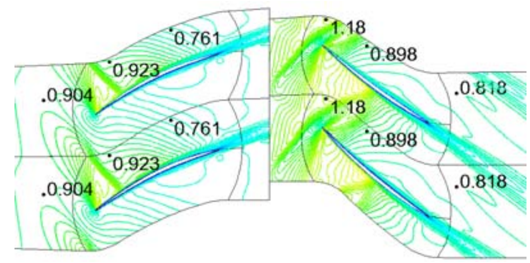

(b) 50% span

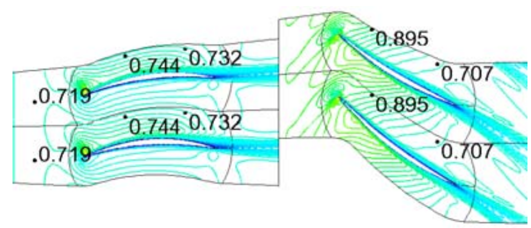

(c) 10% span

Fig. 14 Relative Mach number contours at the design point of civil CRF

For the military contra-stage, the tip clearances of the front and aft rotors are 0.95 mm and 0.80 mm respectively, equivalent to 0.50% of the mean span of each rotor. The map of simulated military contra-stage performance is shown in Fig. 15, which is much steeper in efficiency variation compared to that of the civil contra-stage. At the design point, in despite of the full-span relative supersonic flow at the aft rotor entry, this contra-stage still produce a total pressure ratio of 3.496 with an acceptable simulated isentropic efficiency of 84%, alternatively a polytropic efficiency of 86.3%, obtaining a reasonable stall margin of 14%, at a mass flow of 64.46 kg/s. Also, it presents a satisfying off-design performance. For instance, the peak isentropic efficiency achieved under the (0.95, -0.95) speed is 86.2%, corresponding to a polytropic efficiency of 88.2%, associated with a stall margin of 13.2% at this point. The shock structure of central S_2 surface projected on the meridional plane is presented in Fig. 16. Different from the front rotor, which is a conventional transonic rotor and its passage shock eliminates at 40% span, the aft rotor is a full-span relative supersonic rotor in which both the leading edge shock and the passage shock extend from the casing to the hub, as shown in Fig. 16. The three dimensional shock series structure is also illustrated in Fig. 17, by relative Mach number contours in the blade-to-blade planes. It is indicated that the oblique shocks propagating from the leading edge of the aft rotor impinge on the adjacent blade suction surface, then reflect to the pressure surface, then reflect again. As a result, a wide region encompassing the shock series is established, as shown also in Fig. 16. The Mach number is greatly decreased throughout those oblique shocks, and the resultant passage normal shock is substantially weak. It is interesting to point out that, although no boundary layer controls were employed, no separation region was found for the reason of the particular shock series aforementioned. Furthermore, the shock series proved to be an efficient compression system. Towards the hub sections within 6% span of the aft rotor, as shown in Fig. 16, a local low-velocity but not separated region, resulting from shock-boundary layer interaction, is presented after the passage shock impingement point. Along the performance curve of the speed (1.0, -1.0), as the stage back pressure increases, the aft rotor passage shock moves upstream, and the shock impingement point at the hub still locates within the cover portion of the passage, while the low-velocity region shrinks rapidly. It is believed that the smaller hub curvature at the front of the passage is responsible for the shrinking.

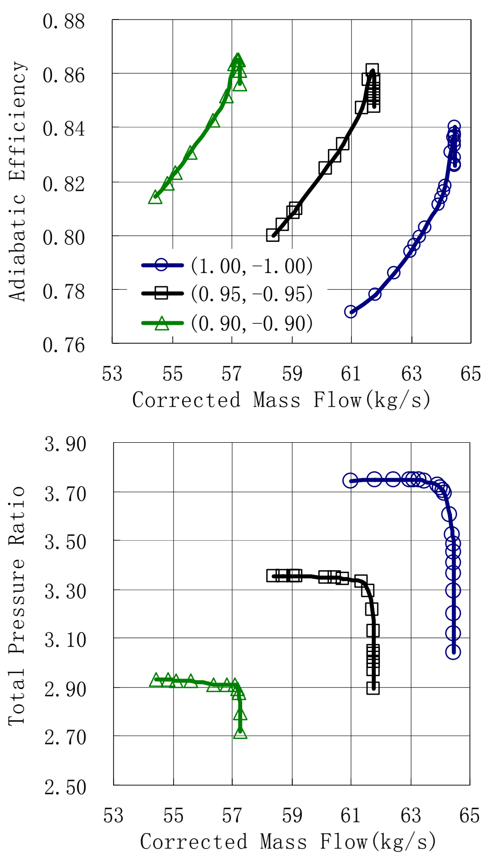

Fig. 15 Corrected military contra-stage performance map

As empirical ideas of the design parameters, a contra-stage designed to produce a pressure ratio of 3.0 could obtain a measured isentropic efficiency 87% at the tip speeds of (442 m/s, -351m/s), employing inlet guide vane and aspiration on the aft rotor [13]. Herein the numerical investigation reveals that a pressure ratio of 3.5 could be achieved by the vaneless, non-aspirated contra-stage at an isentropic efficiency of 84%, with tip speeds of (500 m/s, -391 m/s).

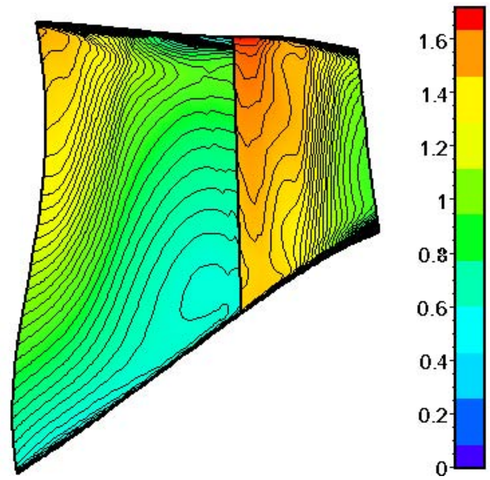

Fig. 16 Contours of relative Mach number on central S2 surface projected on meridional plane

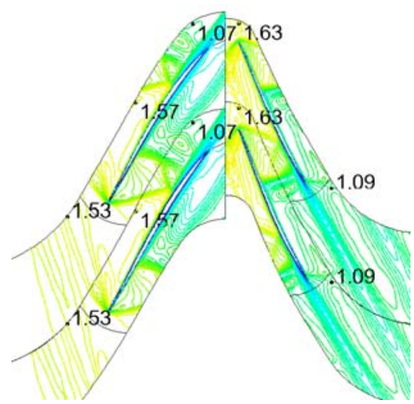

(a) 90% span

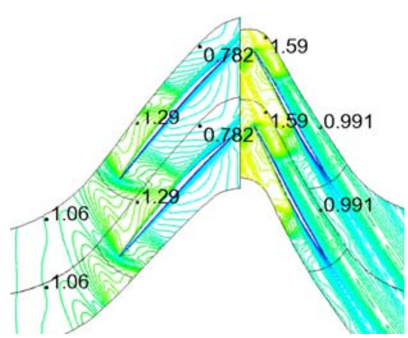

(b) 50% span

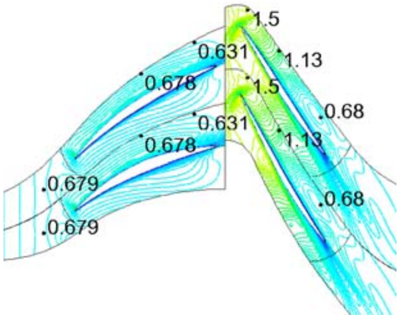

(c) 10% span

Fig. 17 Relative Mach number contours of the military contra-stage at the design point

DISCUSSION OF MASS FLOW CHARACTERISTICS OF TWO KINDS OF CRF

The simulated rotors and stage pressure ratio–mass flow performances of civil and military CRFs are illustrated in Fig. 18. Both the aft rotors of CRFs do not exhibit the choking operation features, and the total pressures are weak functions of the mass flow, in other words, both presented as flat curves of total pressure ratio against the mass flow as indicated. The choking mass flow of the aft rotor is just the choking mass flow of the contra-stage.

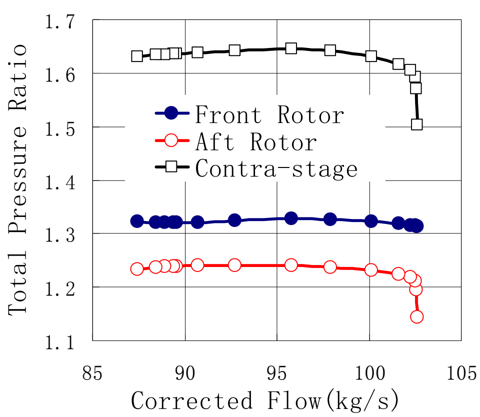

(a) Civil rotors and contra-stage

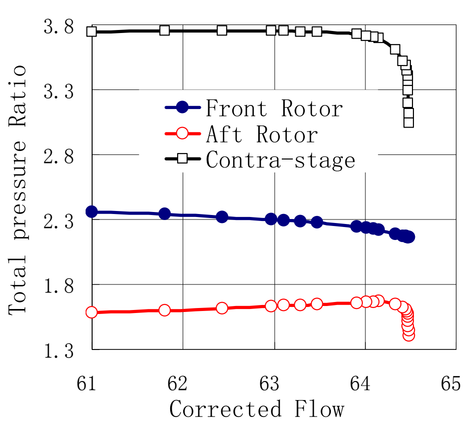

(b) Military rotors and contra-stage

Fig. 18 Simulated pressure ratio–mass flow performances

The shock structures of the civil and military fans at the 90% span under the speed of (1.0,-1.0) in different mass flow conditions are pictured in Fig. 19 and 20 respectively. At near-choke condition, the aft rotor of each contra-stage is choking and determines the choking mass flow of the contra-stage. As the back pressure increases, the passage shock of the aft rotor moves upstream while the shock series of the front rotor does not vary until the knee in the contra-stage speed line is arrived where the flow just begins to drop. Therefore the stage mass flow characteristics before the knee are determined solely by the aft rotor.

The two contra-stages both have a higher stage stall margin than the conventional stages. At the stall point, for the civil test fan of low pressure ratio, both the front and aft rotors are stall and the shocks are detached, correspondingly, for the military fan of high pressure ratio, only the aft rotor is stall and it determines the stage stall point.

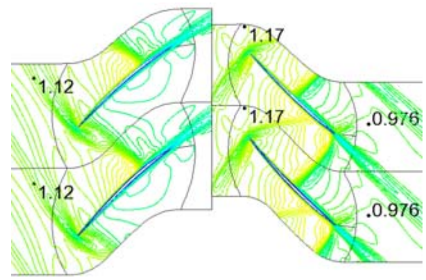

(a) near choke

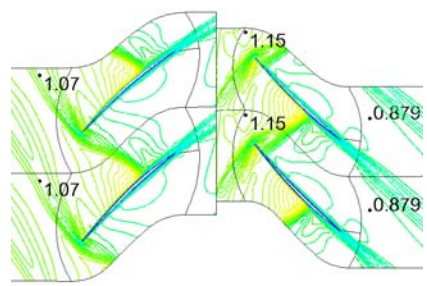

(b) peak efficiency

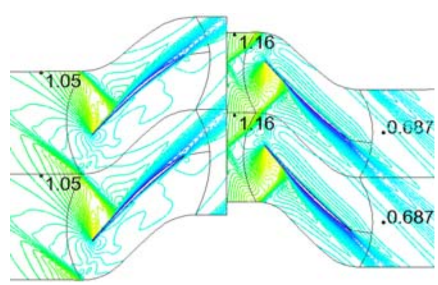

(c) near stall

Fig. 19 Relative Mach number contours of the civil contra-stage at the 90% span on the design speed in different mass flow conditions

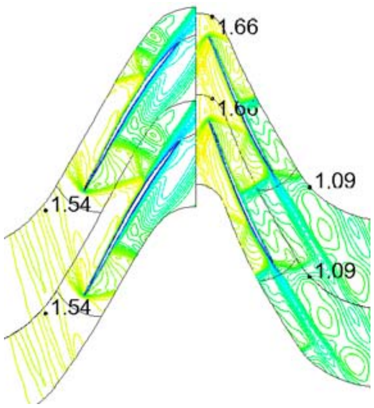

(a) near chock

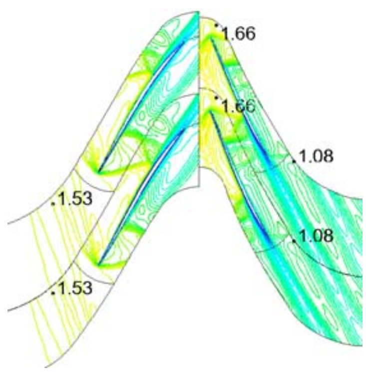

(b) peak efficient

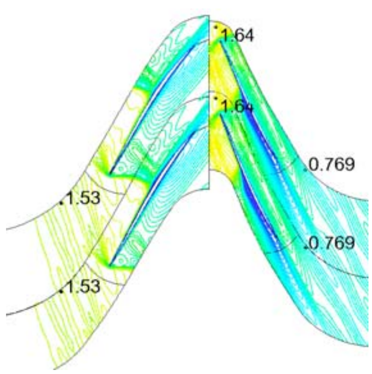

(c) near stall

Fig. 20 Relative Mach number contours of the military contra-stage at the 90% span on the design speed in different mass flow conditions

CONCLUSIONS

(1) Two types of counter-rotating fans for the civil and military applications respectively, both vaneless and non-aspirated, with quite different aerodynamic characteristics, were designed and numerically investigated. The pressure ratios are 1.60 and 3.50 respectively, and the tip speeds are (300 m/s, -222 m/s) and (500 m/s, -391 m/s).

(2) The losses of a contra-stage originate primarily from the aft rotor. When the rotating speed of the front rotor is held constant, the losses increase rapidly as the rotating speed of the aft rotor increases, while the losses from the front rotor is not sensitive to the speed changes.

(3) The contra-stage exhibits a higher thoughflow capacity compared to the conventional rotor-stator stage. The advantage becomes more prominent as the design pressure ratio decreases, and weaker as the design pressure ratio increases. It can be explained in terms of shock losses increasing in the aft rotor.

(4) The shock series presented in the aft rotor of a high pressure ratio contra-stage, featured as multi-reflected inclined shocks coupled with a weak normal passage shock, can cause no separation there, and serve as an efficient compression system.

(5) A contra-stage has a higher stall margin than a conventional stage. Different design pressure ratios lead to obviously different near stall characteristics of contra-stages; at the other end of the iso-speed line, the aft rotor always dominates the choking performance of it.

REFERENCES

[1] Wennerstrom, A. J., and Frost, G. R., 1976, “Design of a 1500ft/sec, transonic, high-through-flow, single-stage axial-flow compressor with low hub/tip ratio,” AFARL-TR-76-59, AD-B016386.

[2] Wennerstrom, A. J., and Forst, G. R., 1974, “Design of a Rotor Incorporating Splitter Vanes for a High Pressure Ratio Supersonic Axial Compressor Stage,” ARL-TR-74-0110.

[3] Merchant, A. A., 1999. “Design and Analysis of Axial Aspirated Compressor Stages,” PHD thesis, Massachusetts Institute of Technology, Cambridge.

[4] Brent, J. A. and Clemmons, D. R., 1974, “Single-stage Experimental Evaluation of Tandem-Airfoil Rotor and Stator Blading for Compressors,” Part VIII - Final Report. NASA CR-134713.

[5] Yonug, R. H., 1951, “Contra-rotating axial fans,” J. Instn. Heat. Vent. Eng., 18.

[6] Johnsen, L. J. and Fessler, T. E., 1957, “Experimental Investigation of Performance of Single-Stage Transonic Compressor with Guide Vanes Turning Counter to Direction of Rotor Whirl,” NACA RM E57B04.

[7] Final Report on Compressor Portion of Turboaccelerator Crcle Evaluation and Experimental Verification Program. PWA-2833, Pratt & Whitney Aircraft, June 1966.

[8] Sabel, E. J., and Sabatiuk, A., 1957, “Turbojet Engine Development: Design of Phase I Compressor,” Curtiss-Wright Corporation, C. W. R. Report NO. 501.

[9] Sabel, E. J., and Sabatiuk, A., 1957, “Turbojet Engine Development: Phase II Compressor Test Results,” Curtiss-Wright Corporation, C. W. R. Report NO. 502.

[10] Wennerstrom, A. J., 1990, “Highly Loaded Axial Flow Compressors: History and Current Developments,” ASME Journal of Turbomachinery, 112(4), pp. 567-578.

[11] Law, C. H. and Wennerstrom, A. J., 1987, “Performance of two transonic compressor rotors incorporating inlet counterswirl,” ASME Journal of turbomachinery, 109(1), pp. 142-149.

[12] Shama, P. B., Jain, Y. P., Jha, N. K., et al. 1985, “Stalling behavior of a counter-rotating stage,” 7th International Symposium on Air Breathing engines, No.85-7087.

[13] Kerrebrock, J. L., Epstein, A. H., Merchant, A. A., et al. 2008, “Design and test of an aspirated counter-rotating fan,” ASME Journal of turbomachinery, 130(2), pp. 198-206.

[14] Donald, H. T., 2004, “Parametric Study of a Mach 2.4 Transport Engine with Supersonic Through-Flow Rotor and Supersonic Counter-Rotating Diffuser (SSTR/SSCRD),” NASA TM-2004-213139.

[15] Ryojiro Minato, Toyohiko Ota, Kiyoshi Fukutomi, et al. 2007, “Development of Counter Rotating Axial Fan Turbojet Engine for Supersonic Unmanned Plane,” Paper No. AIAA-2007-5023.

[16] Lieblein, S., Schwenk, F. C., and Broderick, R. L., 1953, “Diffusion Factor for Estimating Losses and Limiting Blade Loadings in Axial-flow-compressor Blade Elements,” NACA RM E53D01.

[17] Miller, G. R., Lewis, G. W., and Hartmann, M. J., 1961, “Shock losses in transonic compressor blade rows,” ASME Journal of Engineering for Power, 83(4), pp. 235-242..

[18] Xiao-He Yang, Peng Shan, 2010, “Integrative Design Method of Fan and Axial-Centrifugal Compressors,” Transactions of Chinese Society of Aeronautics and Astronautics, Journal of Aerospace Power, 25(2), pp. 443-450. (In Chinese).

[19] Frost, G. R. and Wennerstrom, A. J., 1973, “The Design of Axial Compressor Airfoils Using Arbitrary Camber Lines,” ARL 73-0107, AD 765165.

[20] NUMECA Int., 2000, “Numeca’s Flow Integrated Environment for Turbomachinery and Internal Flows,” User Manual, Numeca Int., Brussels, Belgium.

[21] Spalart, P. R., and Allmaras, S. R., 1992, “A One-equation Turbulence Model for Aerodynamic Flows,” AIAA Paper 92-0439.